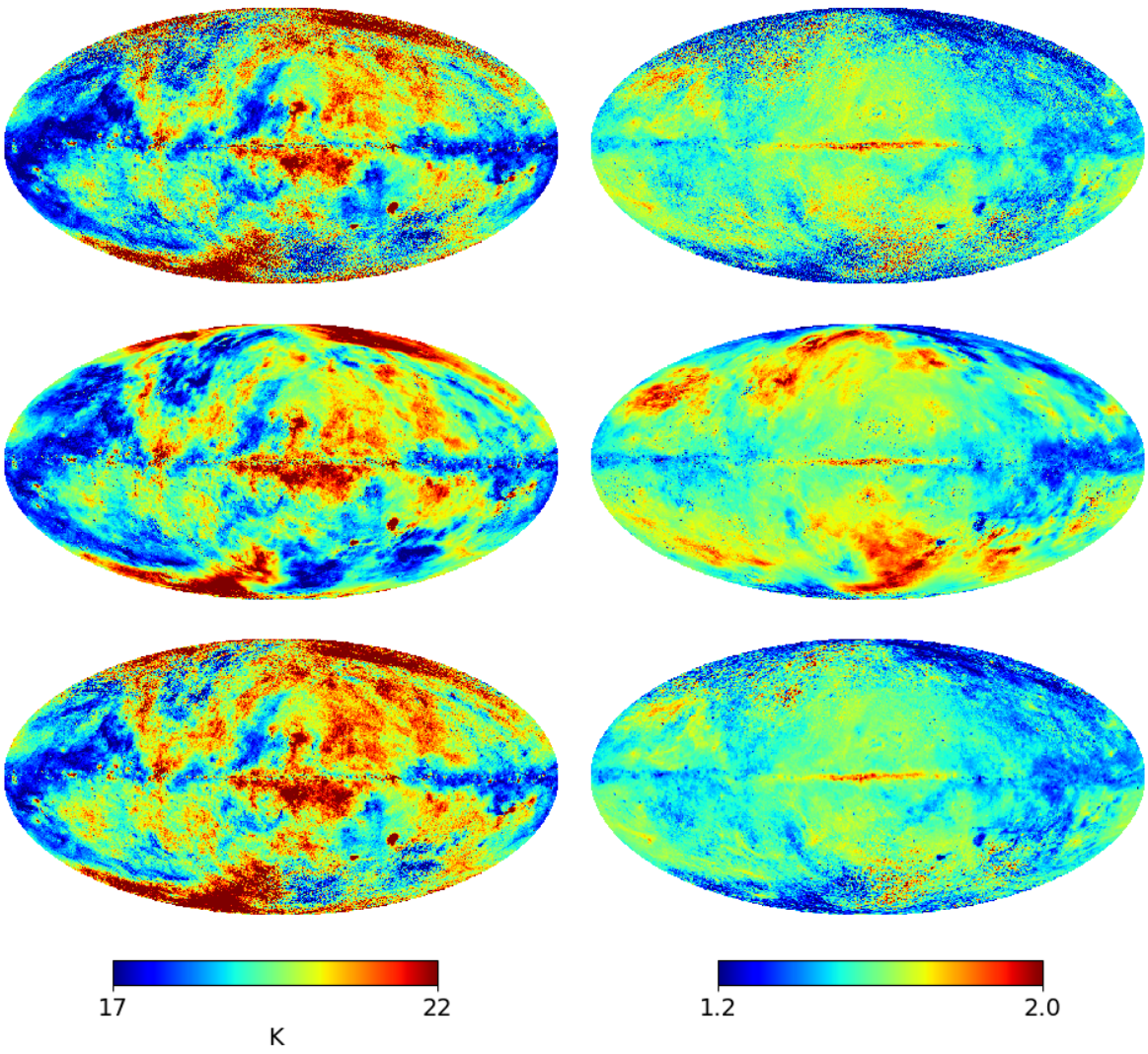

Figure 1: Thermal dust MBB temperatures (*left*) and spectral indices (*right*) as calculated by `premise` (*top*), GNILC (*middle*), and 2013 (*bottom*).

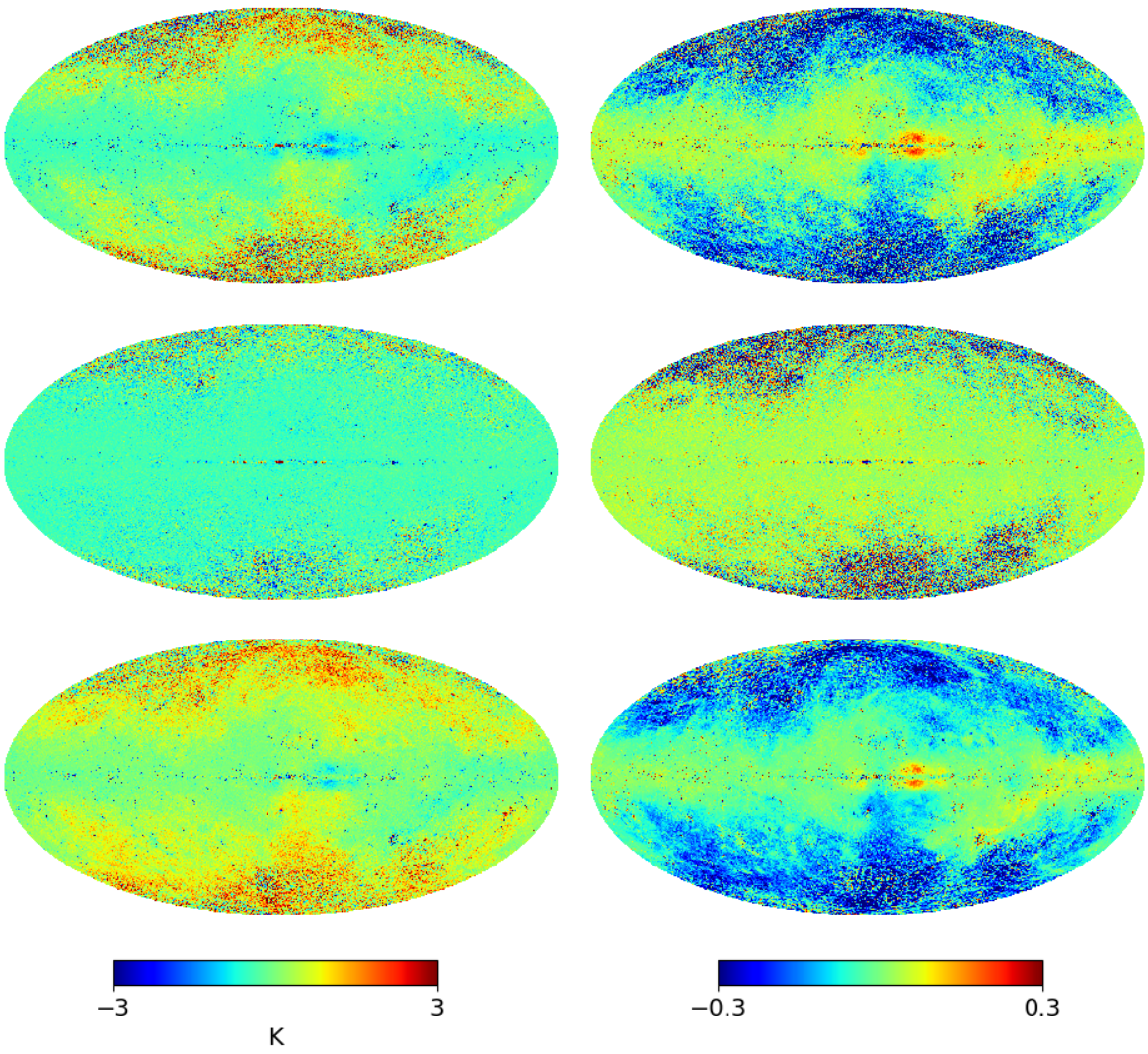

Figure 2: Differences in thermal dust MBB temperatures (*left*) and spectral indices (*right*). `premise` minus GNILC (*top*), `premise` minus 2013 (*middle*) and 2013 minus GNILC (*bottom*).

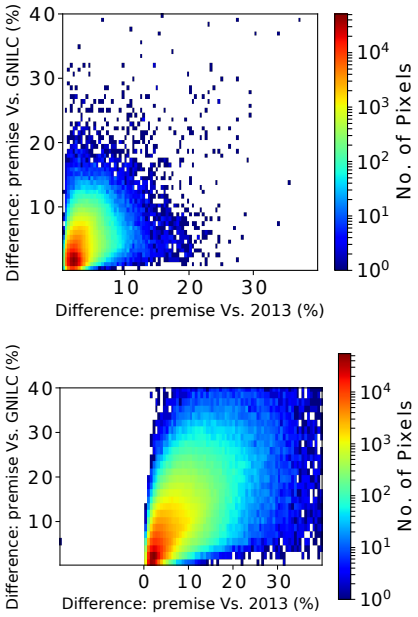

Figure 3: Absolute percentage difference between the `premise` and GNILC temperature (*top*)/spectral index (*bottom*) values against the absolute percentage difference between the `premise` and 2013 temperature/spectral index values.

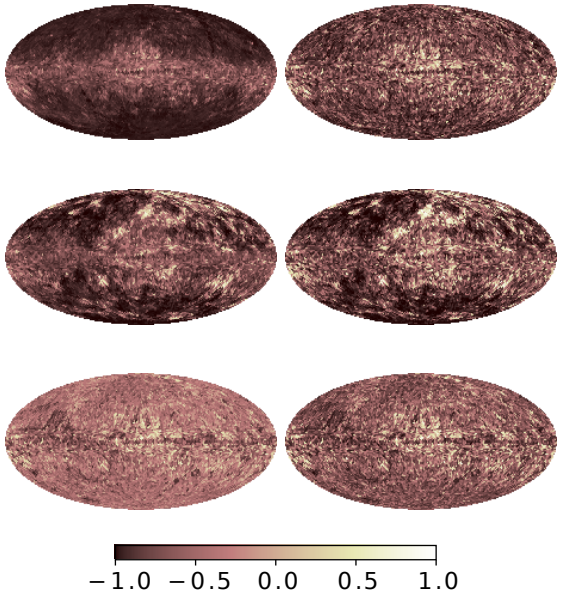

Figure 5: Temperature and spectral index correlation maps for `premise` parameters *(top)*, GNILC parameters *(middle)*, and 2013 parameters (*bottom*). The colour scale gives the correlation coefficient values. The left column shows the parameters at their original resolutions, whilst in the right column the correlation maps are made from parameters smoothed to 30 arcmin.

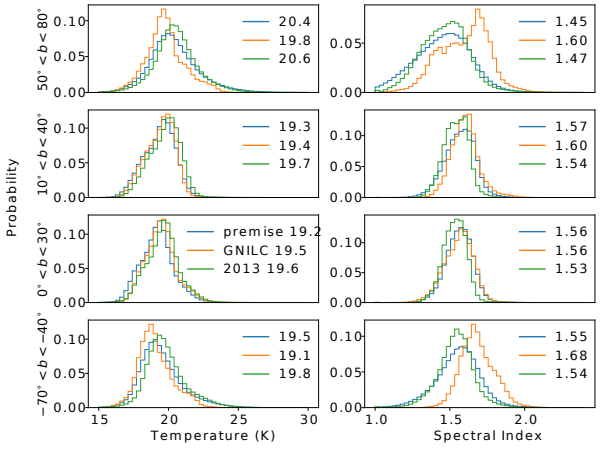

Figure 4: Histogram comparison of `premise` (blue), 2013 (green), and GNILC (red) temperatures (*left*) and spectral indices (*right*) for different strips in Galactic latitude.

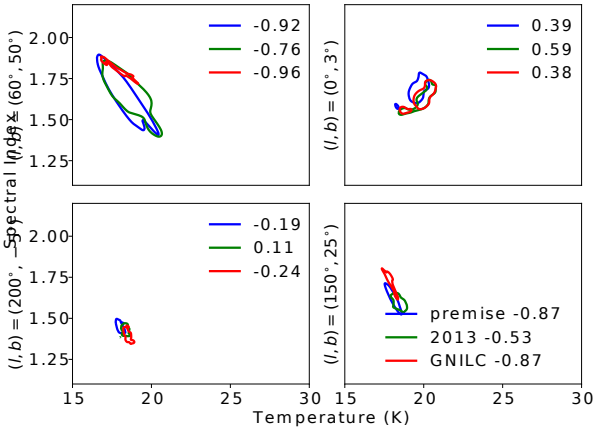

Figure 6: Contour plots of temperature and spectral index for `premise`, GNILC, and 2013. The one-sigma level contour is shown for a two degree radius circle of pixels centred at various coordinates.

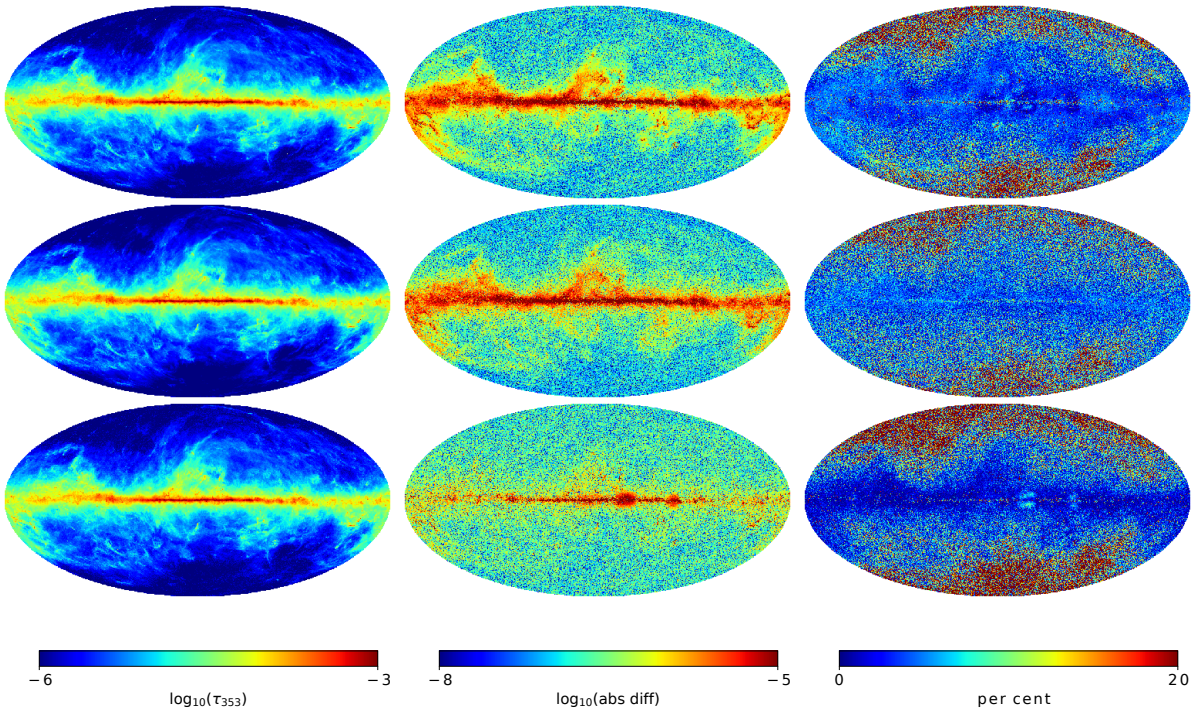

Figure 7: *Left column*: Optical depth at 353 GHz as calculated by `premise` (*top*), GNILC (*middle*), and 2013 (*bottom*). *Middle column*: Differences between the optical depth at 353 GHz estimates, `premise` minus GNILC (*top*), `premise` minus 2013 (*middle*), and 2013 minus GNILC (*bottom*). *Right column*: Percentage differences between the optical depth at 353 GHz estimates.

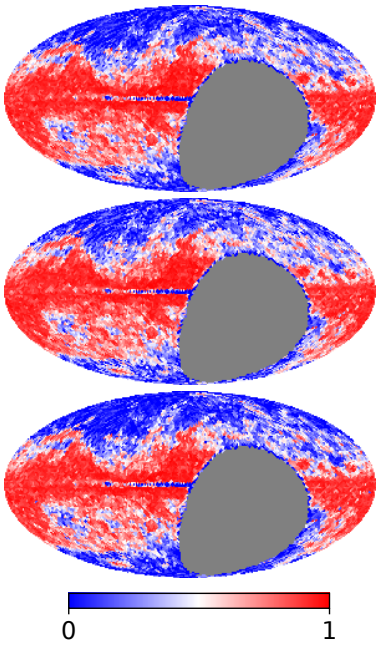

Figure 8: E(B-V) and τ_{353} correlation maps for `premise` parameters *(top)*, GNILC parameters *(middle)*, and 2013 parameters (*bottom*). The colour scale gives the correlation coefficient values.

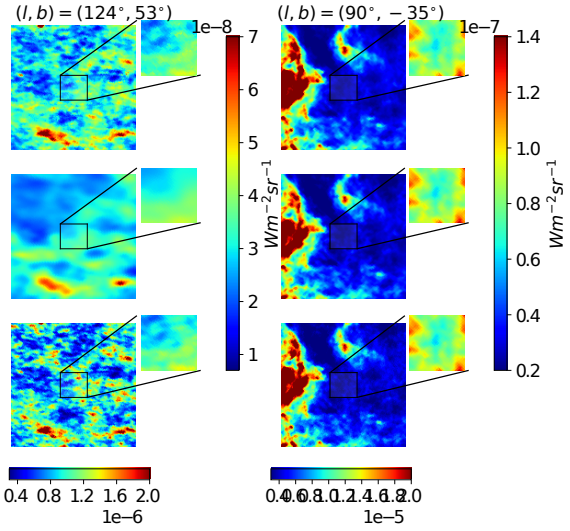

Figure 10: τ_{353} maps of five-by-five degrees within two different regions for `premise`, GNILC, and 2013 *(from top to bottom)*. The insets show zoomed-in images of the central one-by-one degree regions of each map and display the equivalent radiance map for each method. The central coordinate of each map is given above each column.

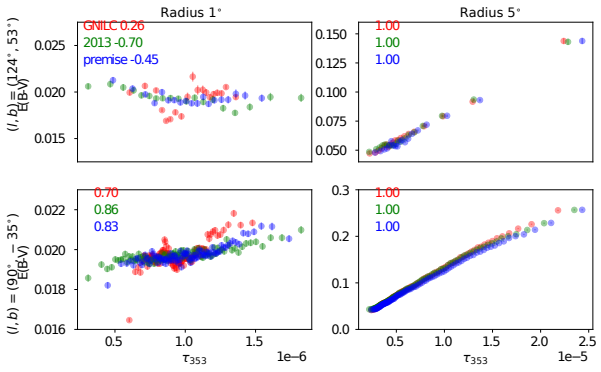

Figure 9: E(B-V) vs. τ_{353} scatter plots for two different regions and two different angular scales.

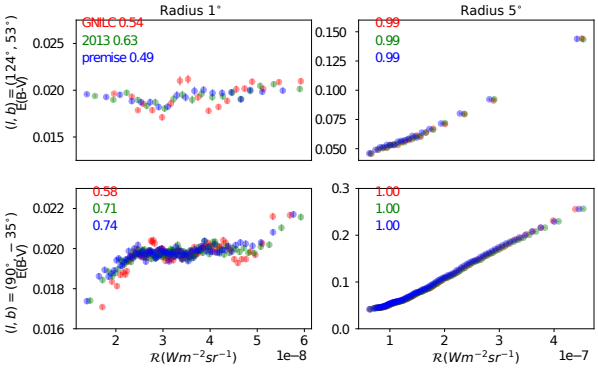

Figure 11: E(B-V) vs. radiance scatter plots for two different regions and two different angular scales.

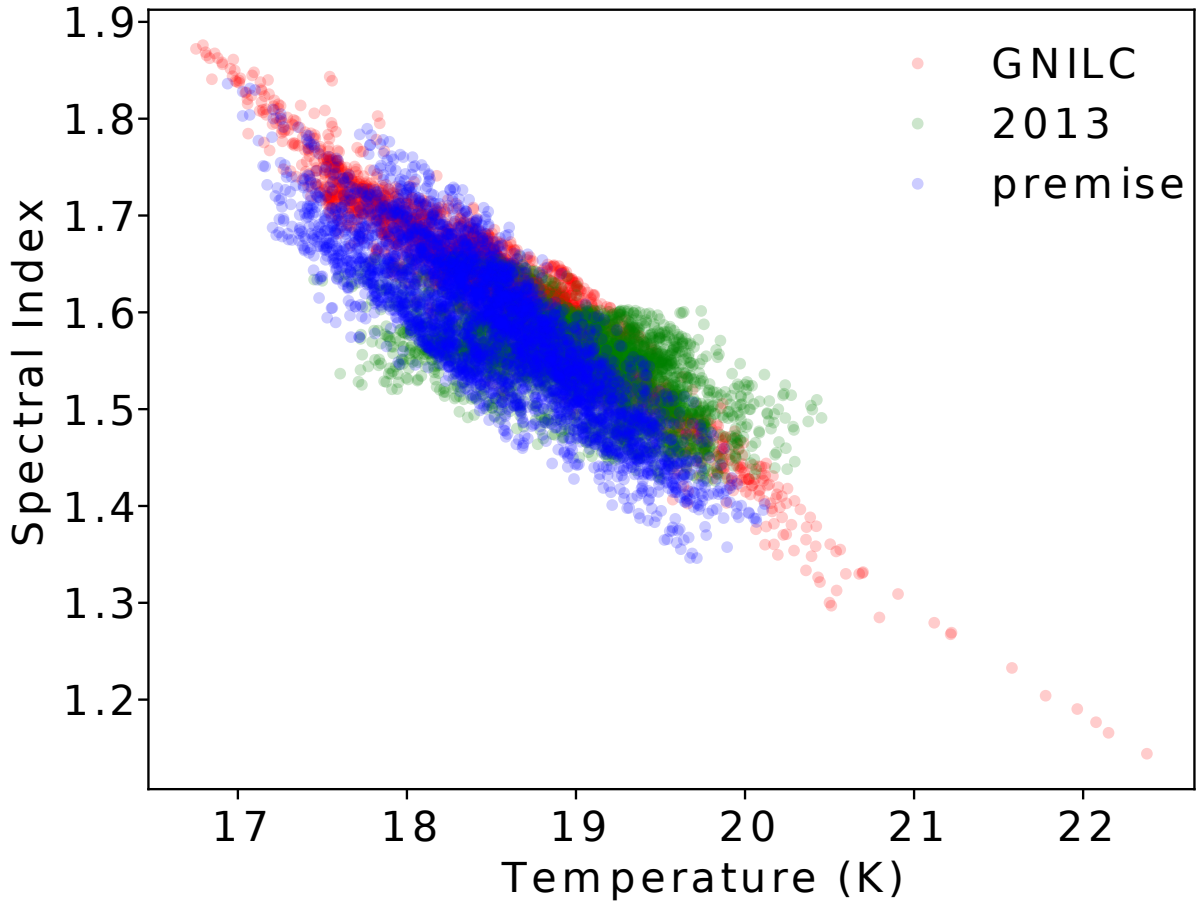

Figure 12: Temperature vs. spectral index scatter plot for the pixels contained within the one degree radius circle centred at $(l, b) = (90°, -35°)$.

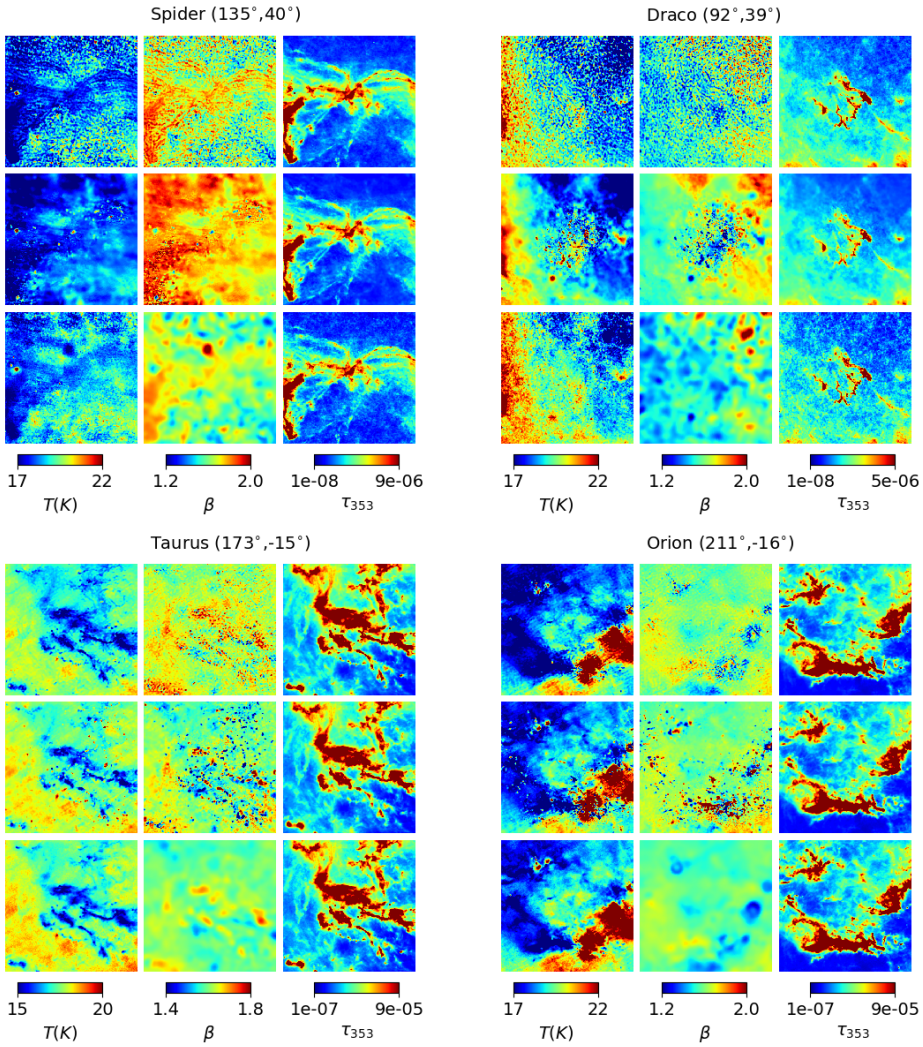

Figure 13: The MBB parameters for four molecular clouds as calculated by `premise` *(top)*, GNILC *(middle)*, and 2013 *(bottom)*. The images are all 12x12°.

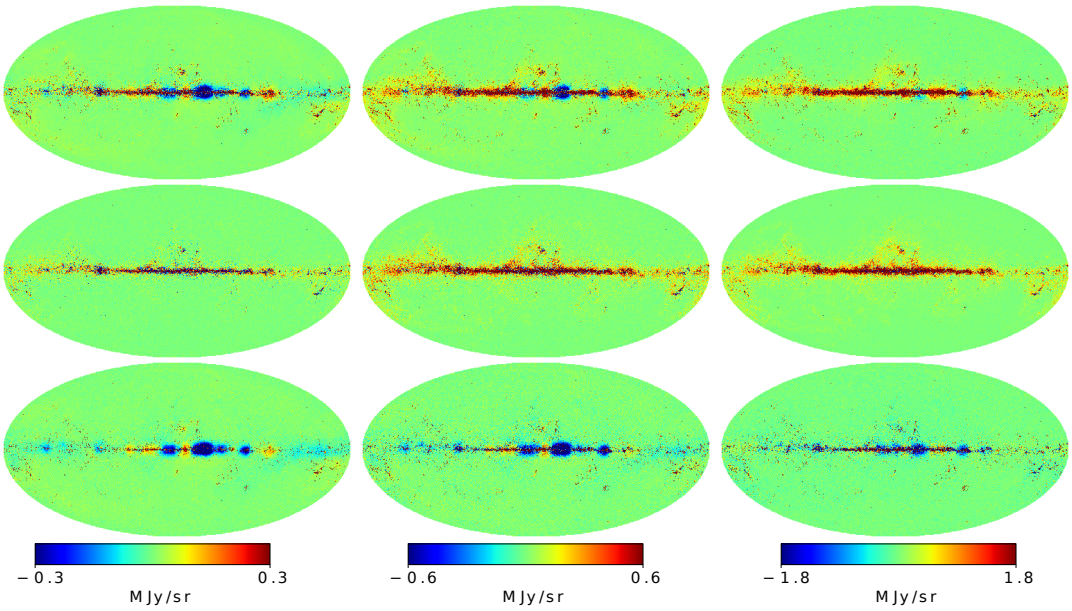

Figure 14: Difference maps between the two thermal dust intensity estimates at each frequency: 353, 545, and 857 GHz *(left to right)*. *(Top)* $\text{premise}_{\text{MBB}}$ - $\text{GNILC}_{\text{MBB}}$, *(middle)* $\text{premise}_{\text{MBB}}$ - 2013_{MBB}, *(bottom)* 2013_{MBB} - $\text{GNILC}_{\text{MBB}}$.

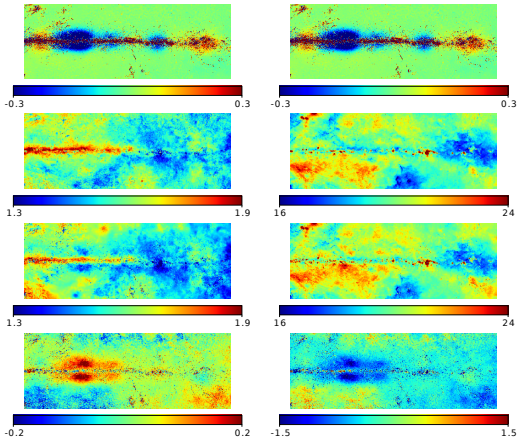

Figure 15: *Left:* Cartesian projection of the central Galactic plane region of the `premise` 353 GHz dust estimate minus GNILC 353 GHz dust estimate (*top*), `premise` spectral index map (*upper middle*), GNILC spectral index map (*lower middle*), `premise` - GNILC spectral index map (*lower middle*). *Right:* Same as the left, but for temperature.

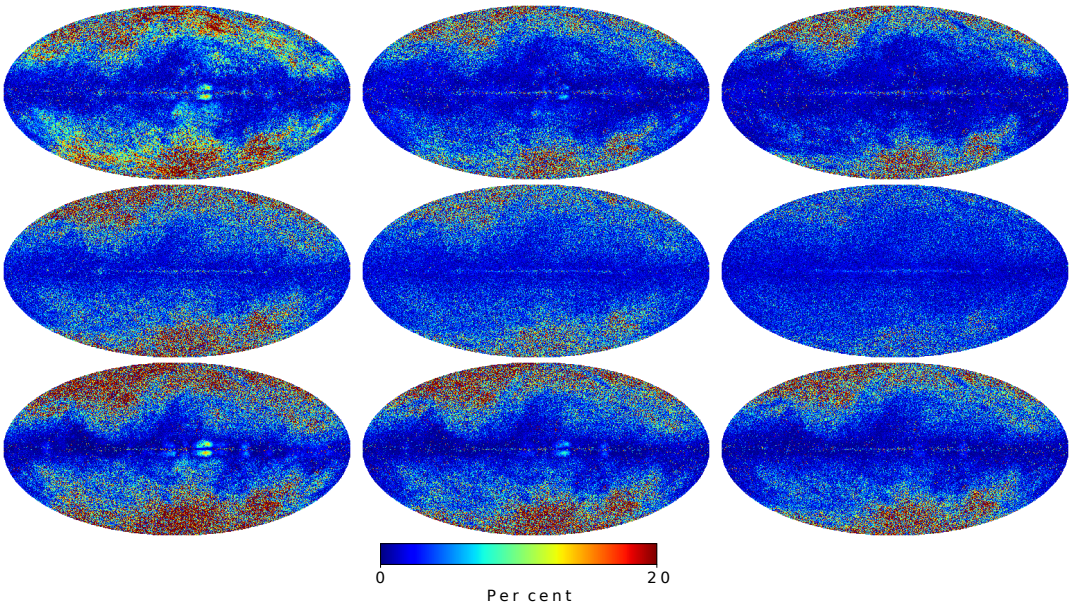

Figure 16: Percentage difference maps between the MBB thermal dust intensity estimates at each frequency: 353, 545, and 857 GHz *(from left to right)*. *(Top)* $\text{premise}_{\text{MBB}}$ - $\text{GNILC}_{\text{MBB}}$, *(middle)* $\text{premise}_{\text{MBB}}$ - 2013_{MBB}, *(bottom)* 2013_{MBB} - $\text{GNILC}_{\text{MBB}}$.

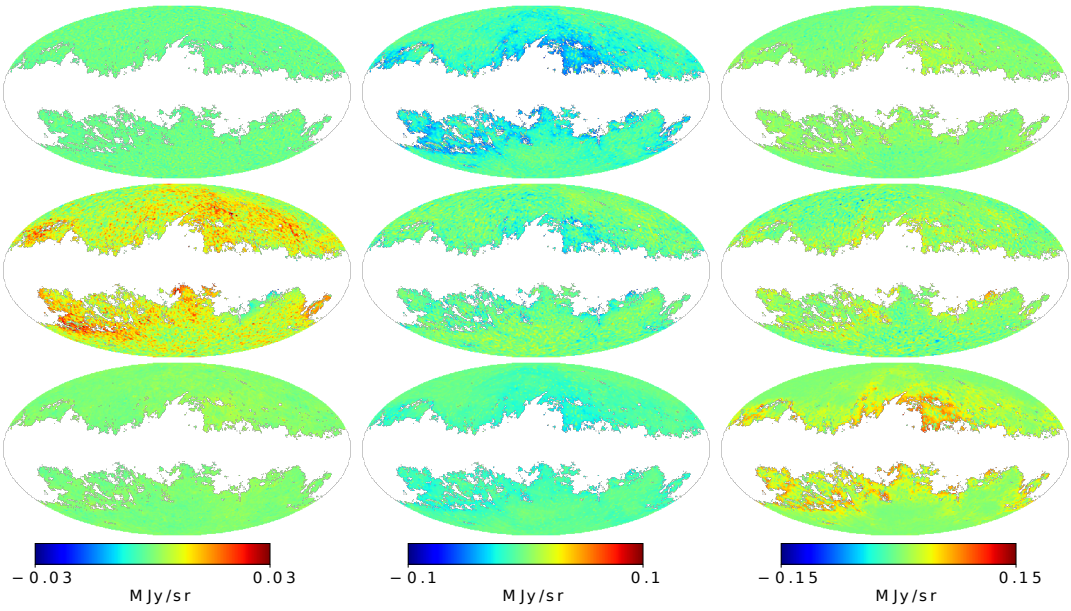

Figure 17: CIBA plus instrumental noise maps at 1° resolution made by (*Top*) $\text{premise}_{\text{MBB}}$, (*middle*) $\text{GNILC}_{\text{MBB}}$, and (*bottom*) 2013_{MBB} at 353, 545, and 857 GHz (*from left to right).*

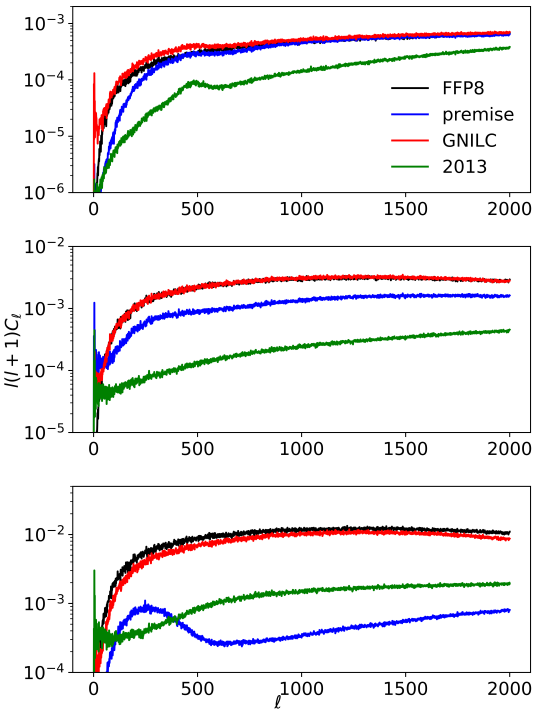

Figure 18: Power spectra of the CIBA plus instrumental noise estimates alongside the FFP8 simulations at 353, 545, and 857 GHz (*top to bottom).*

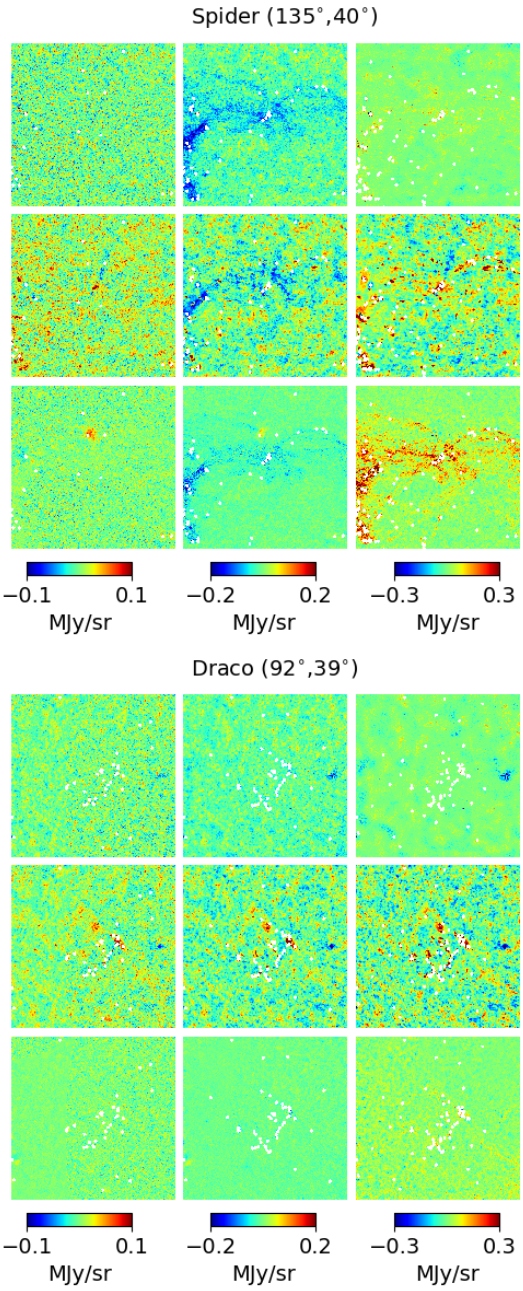

Figure 19: The CIBA plus instrumental noise estimates at 353, 545 and 857 GHz *(from left to right)* for two molecular clouds as calculated by `premise` *(top)* , GNILC *(middle)* and 2013 *(bottom).* Point sources within have been masked out using the *Planck* HFI masks.